Single Shot Characterization of High Transformer Ratio Wakefields in Nonlinear Plasma Acceleration

R. Roussel, G. Andonian, W. Lynn, K. Sanwalka, R. Robles, C. Hansel, A. Deng, G. Lawler, J. B. Rosenzweig, G. Ha, J. Seok, J. G. Power, M. Conde, E. Wisniewski, D. S. Doran, and C. E. Whiteford

Phys. Rev. Lett. **124**, 044802 — Published 31 January 2020

DOI: 10.1103/PhysRevLett.124.044802

Single-Shot Characterization of High Transformer Ratio Wakefields in Nonlinear Plasma Acceleration

R. Roussel,* G. Andonian, W. Lynn, K. Sanwalka, R. Robles, C. Hansel, A. Deng, G. Lawler, and J.B. Rosenzweig

Department of Physics and Astronomy, University of California, Los Angeles, California 90095, USA

G. Ha, J. Seok, J. G. Power, M. Conde, E. Wisniewski, D. S. Doran, and C. E. Whiteford

Argonne National Laboratory, Argonne, Illinois 60439, USA

(Dated: November 13, 2019)

Abstract

Plasma wakefields can enable very high accelerating gradients for frontier high energy particle accelerators, in excess of 10 GeV/m. To overcome limits on single stage acceleration specially shaped drive beams can be used in both linear and nonlinear plasma wakefield accelerators (PWFA), to increase the transformer ratio, implying that the drive beam deceleration is minimized relative to acceleration obtained in the wake. In this Letter, we report the results of a nonlinear PWFA, high transformer ratio experiment using high-charge, longitudinally asymmetric drive beams in a plasma cell. An emittance exchange process is used to generate variable drive current profiles, in conjunction with a long (multiple plasma wavelength) witness beam. The witness beam is energy-modulated by the wakefield, yielding a response that contains detailed spectral information in a single-shot measurement. Using these methods, we generate a variety of beam profiles and characterize the wakefields, directly observing transformer ratios up to $\mathcal{R} = 7.8$. Furthermore, a spectrally-based reconstruction technique, validated by 3D particle-in-cell simulations, is introduced to obtain the drive beam current profile from the decelerating wake data.

The development of beam-based plasma wakefield acceleration (PWFA) schemes has provided a potential path to extremely compact high energy accelerators, due to its ability to sustain accelerating gradients well in excess of 10 GeV/m [1]. PWFA uses a highly energetic, high charge bunched beam known as the drive, to excite a nonlinear plasma density wave. The fields in this wave are used to accelerate a second bunch, known as the witness, placed collinearly behind the drive. While this provides a substantial enhancement in peak accelerating field over current state-of-the-art acceleration schemes, improvements to energy transfer from the drive bunch to the witness, using bunch shaping, are necessary for reducing drive beam constraints on single stage energy gain.

Energy transfer from the drive beam to the witness is parameterized by the transformer ratio, which is defined as $\mathcal{R} = |W_+|/|W_-|$, the ratio between the maximum accelerating field experienced by the witness $|W_+|$ and the maximum decelerating field found inside the drive $|W_-|$. In the context of linear wakefields, it has been shown [2, 3] that the limit $\mathcal{R} < 2$ exists for longitudinally symmetric beams, and that asymmetric beams, such as a linear ramp profile, can exceed this limit. Further work [4] showed that this idea can be extended by modifying the linear ramp in the beam head region to reach even higher transformer

ratios.

Methods of producing linearly ramped beam profiles include the use of: self-wakefields in dielectric structures [5]; anisochronous dogleg beamlines with nonlinear correction elements [6]; laser pulse stacking at the photocathode; [7] and emittance exchange methods [8]. Emittance exchange (EEX) is a process [9] by which a transverse beam distribution is mapped onto the longitudinal coordinate, a technique which allows flexible longitudinal bunch shaping. EEX may also be used to provide a long, temporally synchronized, witness bunch for single-shot, multi-period wakefield measurements [10].

Recent methods have been used to perform detailed study of wakefields with high transformer ratios in collinear accelerator schemes including dielectric structures [11] and plasmas [12]. In the latter, wakefield measurements were made using shaped drive bunches and a short witness bunch, showing high transformer ratios. However, the laser pulse stacking method of shape generation has an inherent limit in bunch charge achievable, due to space-charge driven degradation of the profile in the photo-cathode. In this Letter we describe experimental measurements that apply the EEX beam shaping technique at moderate energy, mitigating space-charge effects, and providing new tools for wakefield measurements. These beams are employed to characterize plasma wakefield responses from various high-charge, ramped drive bunches, using a single-shot wakefield mapping technique [10] that captures essential elements of the PWFA process and provides insight into the wakefield dependence on bunch shape.

Experiments were conducted at the Argonne Wakefield Accelerator (AWA) at Argonne National Laboratory. A cesium telluride photcathode based, L-band electron gun produced 15 nC bunches with a pulse length of 6 ps and a near uniform transverse distribution [13]. Normal conducting L-band accelerating cavities were then used to accelerate these bunches to 40 MeV. These beams were delivered to the experimental beamline seen in Fig. 1. A transverse mask was used to shape the horizontal projection of the beam, which is subsequently mapped into the longitudinal coordinate with the EEX beamline.

The EEX beamline (Fig. 1a) consists of two dogleg sections separated by a transverse deflecting cavity, and is capable of generating a wide range of longitudinal current distributions [8]. In the EEX process, a beam particle with a horizontal phase space coordinate of (x_i,x'_i) is mapped to a final longitudinal position $z_f = (A + BS_x)x_i$ in the linear approximation [9], where coefficients A, B are functions defining the EEX beam optics, which

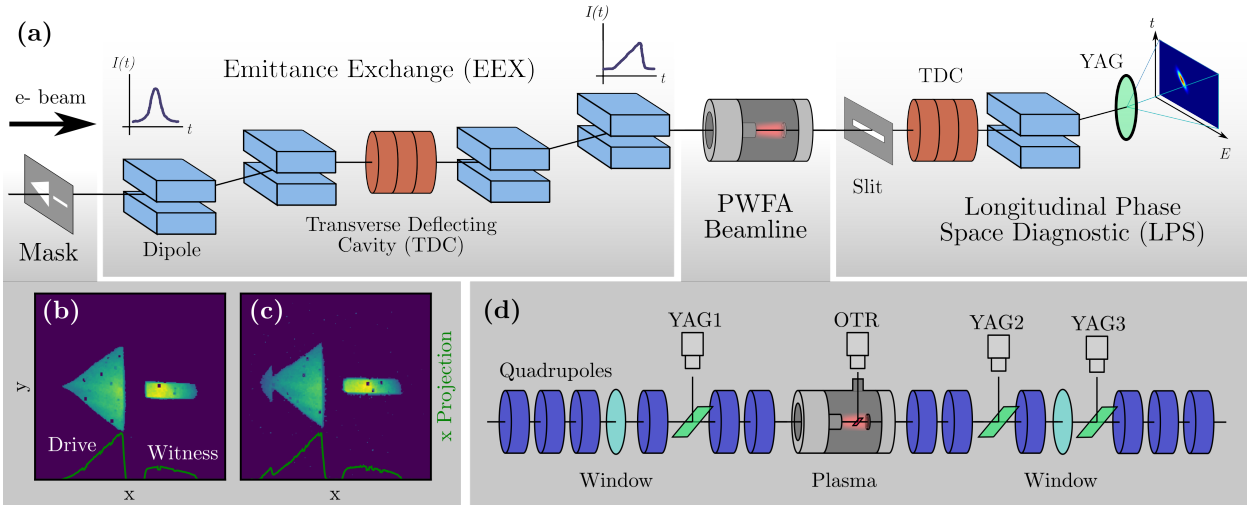

Figure 1. (Color online) Schematic of the beamline at the Argonne Wakefield Accelerator. (a) Beams are delivered to the experimental section consisting of a mask, emittance exchange beamline, PWFA beamline and longitudinal phase space diagnostic. (b-c) Transverse masks were used to shape the transverse beam profile as measured by a straight ahead, transverse YAG screen. Selectable masks shaped the horizontal beam projection to generate a (b) linearly ramped or (c) linear ramp with parabolic head drive beam and a long witness bunch to sample the resulting wakefield. (d) The PWFA beamline is shown with major elements including YAG and optical transition radiation (OTR) screens to view the transverse beam profile.

include transverse dispersion, longitudinal compression and transverse deflection. The term $S_x = dx'/dx$ represents the slope of the $x-x'$ correlation, which can be tuned via quadrupole settings before the EEX mask to optimize the longitudinal profile [14]. Masks were used to shape the horizontal projection of the beam (Fig. 1b, c), generating two drive profiles, a profile ramped over two plasma wavelengths (Fig. 1b) and the same profile but with a parabolic head section added (Fig. 1c). Both masks included a narrow slit used to create a long, low charge witness bunch placed after the shaped drive. After the EEX beamline, the longitudinal profile still has a strong correlation with the vertical dimension. As a result, a long tail after the ramp develops during transport through the PWFA beamline (Fig. 1d) [15], which removes the drive-witness beam separation. This correlation also prevents accurate measurement of the beam current in the longitudinal phase space diagnostic, due to horizontal slitting in the longitudinal phase space diagnostic.

A hollow cathode arc (HCA) plasma source was used to produce a 6 cm long plasma

column with a diameter of 8 mm and a averaged plasma density tunable over the range $n_0 = 0.3 - 1.3$ x 10^{14} cm^{-3} [16]. Argon gas was injected between two concentric tantulum tubes which were heated to 2000 K, creating a thermal electron current high enough to reach the discharge arc regime without the need for a kV class discharge starter. A 150 V, 200 μs pulse was used to discharge the plasma up to a current of 300 A. The plasma density is tuned using this current as well as an external solenoid employed to confine the plasma electrons. The longitudinal plasma density profile on-axis was characterized using a Langmuir triple probe [17] which allows a simultaneous, time resolved measurement of the plasma temperature and density. Beryllium vacuum windows with a thickness of 125 µm were used to isolate the plasma source from the rest of the accelerator, which required an additional beam waist location on either side of the plasma source to reduce emittance growth due to multiple scattering in the windows [18].

To characterize the wakefield interaction a longitudinal phase space (LPS) diagnostic consisting of a transverse deflecting cavity and a 20° dipole spectrometer was used. The transverse deflecting cavity streaks beam particles in the vertical direction according to their arrival time, while the spectrometer dipole maps the energy distribution onto the horizontal dimension. A horizontal slit, placed directly upstream of the LPS diagnostic, was used to vertically collimate the beam to improve the temporal measurement resolution while reducing spurious energy gain signals from transverse electron motion.

A simulation study informed by beam and plasma measurements was performed using the particle-in-cell (PIC) code WARP [19] in a 2D, co-propagating, cylindrical grid with 150 cells per plasma wavelength to simulate a volume which was 11.6 mm in length and 3 mm in radius. A beam was injected into a uniform plasma that filled the simulation volume with a density of 1.5×10^{14} cm^{-3}. The beam size at the interaction point was constrained by optical transmission radiation spot size measurements [20] and consideration of plasma focusing properties due to a non-adiabatic plasma density ramp A beam was injected into a uniform plasma that filled the simulation volume with a density of 1.5×10^{14} cm^{-3}. In the simulations, the estimated beam emittance was obtained by using measurements of beam size at the Be input window, along with a calculation of rms divergence due to multiple scattering [18]. A 40 MeV linearly-ramped drive beam with a length of 5.4 mm, having short fall length, transverse size $\sigma_x = 200$ µm, normalized emittance of 500 mm-mrad and charge of 1.6 nC was injected into a $n_0 = 1.5 \times 10^{14}$ cm^{-3} plasma. A 4 mm long witness

with the same transverse characteristics as the drive and 0.18 nC of charge was injected afterwards to sample the multi-period wake.

Results of the simulation after the beam has traveled 28 mm into the plasma are shown in Fig. 2 after it has been focused transversely by the plasma and reaches a high enough density to excite the nonlinear blowout regime. The rarefaction boundary is notably off-axis for some distance, collapsing only after the drive current drops to near zero. The beam head expands freely, followed by a transverse pinch point where the ion column starts to form and then a region where uniform focusing fields from the ion column dominate [21]. This can degrade shaped features in the bunch head over long propagation distances. Furthermore, electrons in the main body of the beam may escape the rarefaction region due to slice focusing mismatch in the uniform ion region. Since the nonlinear regime is only established after propagating roughly 3 cm into the plasma, an experimental measurement of the averaged wakefield over the entire plasma channel will be smoothed and lower in amplitude relative to the instantaneous wakefield shown in Fig. 2.

This simulation result shows a non-relativistic blowout of plasma electrons due to the ramped beam. This is evident based on the maximum blowout radius observed r_m, which is substantially smaller than the plasma wavelength (≈ 3 mm)[22]. In this quasi-nonlinear case, the decelerating wakefield inside the drive can be approximated by the linear plasma response outside the bubble [23], while accelerated particles at the rear of the bubble still experience a nonlinear wakefield.

During the experiment, the beam was transported through the plasma source while discharges were triggered at half the repetition rate of the accelerator to acquire alternating plasma-on/plasma-off shots, eliminating systematic variations in the LPS present before the plasma. The measured time-slice energy centroids of the plasma-off shots were averaged as a baseline with statistical error to account for beam jitter and charge fluctuations (Fig. 3a). The baseline beam centroid has a notable longitudinal energy chirp from the EEX shaping process. While a separation between drive and witness is apparent in the raw LPS image (Fig. 3a inset), a long tail behind the drive allows for energy centroid calculation in this region. The beam transported through plasma shows a high energy tail in the drive and a periodic modulation of the witness.

To calculate the energy gain from the plasma interaction (Fig. 3b) we subtract the average baseline centroid from the energy centroid of a single plasma "on" shot. Uncertainty in the

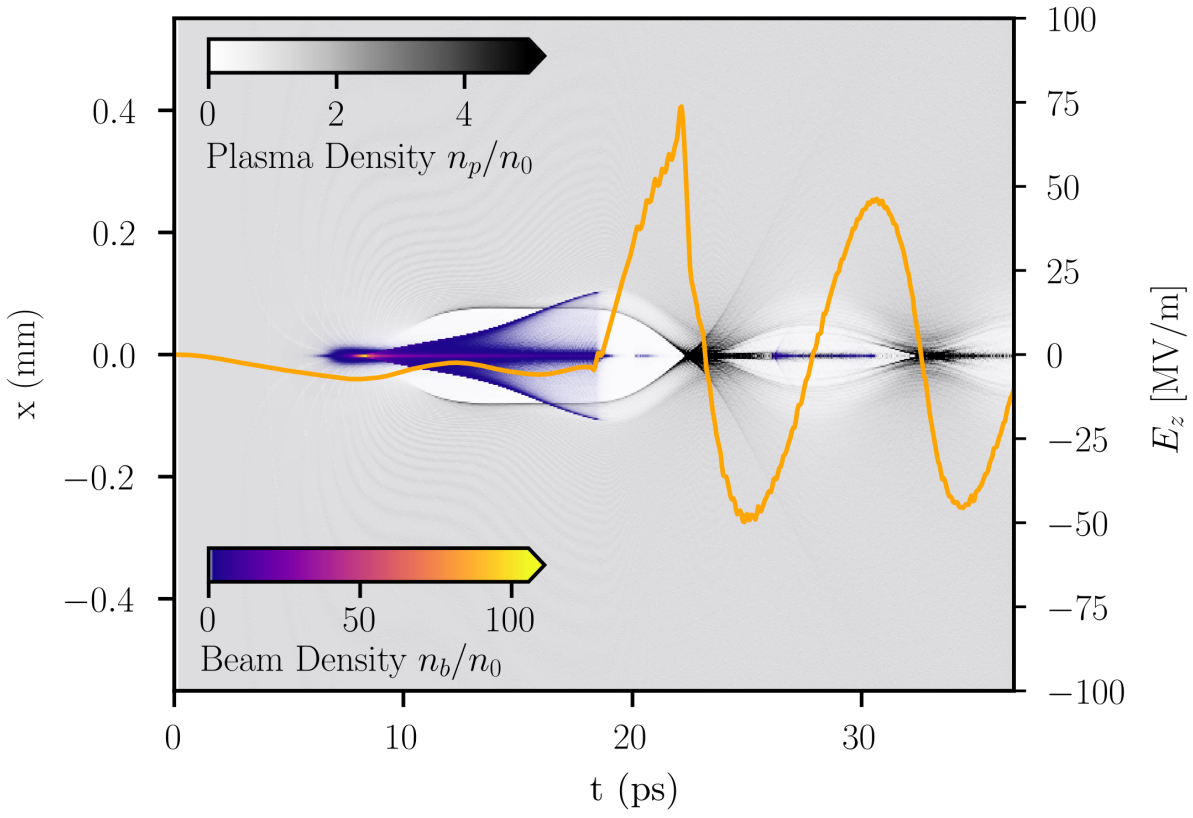

Figure 2. (Color online) Simulation of a linearly ramped drive beam and multi-wavelength witness beam in a n_0 = 1.5 x 10^{14} cm^{-3} plasma. Transverse cross section of plasma and beam densities with on-axis longitudinal wakefield (orange). Maximum blowout radius $r_m < 100$ µm.

baseline energy centroid results in a random energy gain offset for each temporal beam slice (blue shaded region). We calculate an average rms energy gain offset of 35 keV in the region relevant for transformer ratio measurements ($0 < t < 25$ ps).

To quantify the beam current profile at the plasma interaction point, we developed a novel technique for reconstructing the longitudinal current density $\lambda_b(\xi)$ solely from the wakefield response $E(\xi)$ [24],

$$\lambda_b(\xi) \propto -\frac{\epsilon_0}{e}\left[\frac{dE(\xi)}{d\xi} + k_p^2 \int_{-\infty}^{\xi} E(\xi')d\xi'\right], \tag{1}$$

where $\xi = ct - z$ and k_p is the wave number corresponding to the plasma density. This reconstruction assumes a neglectable radial form factor as the beam's transverse size is small relative to the plasma wavelength, and considers the plasma wakefield response inside of the beam to be linear. As discussed before this is an excellent approximation when the

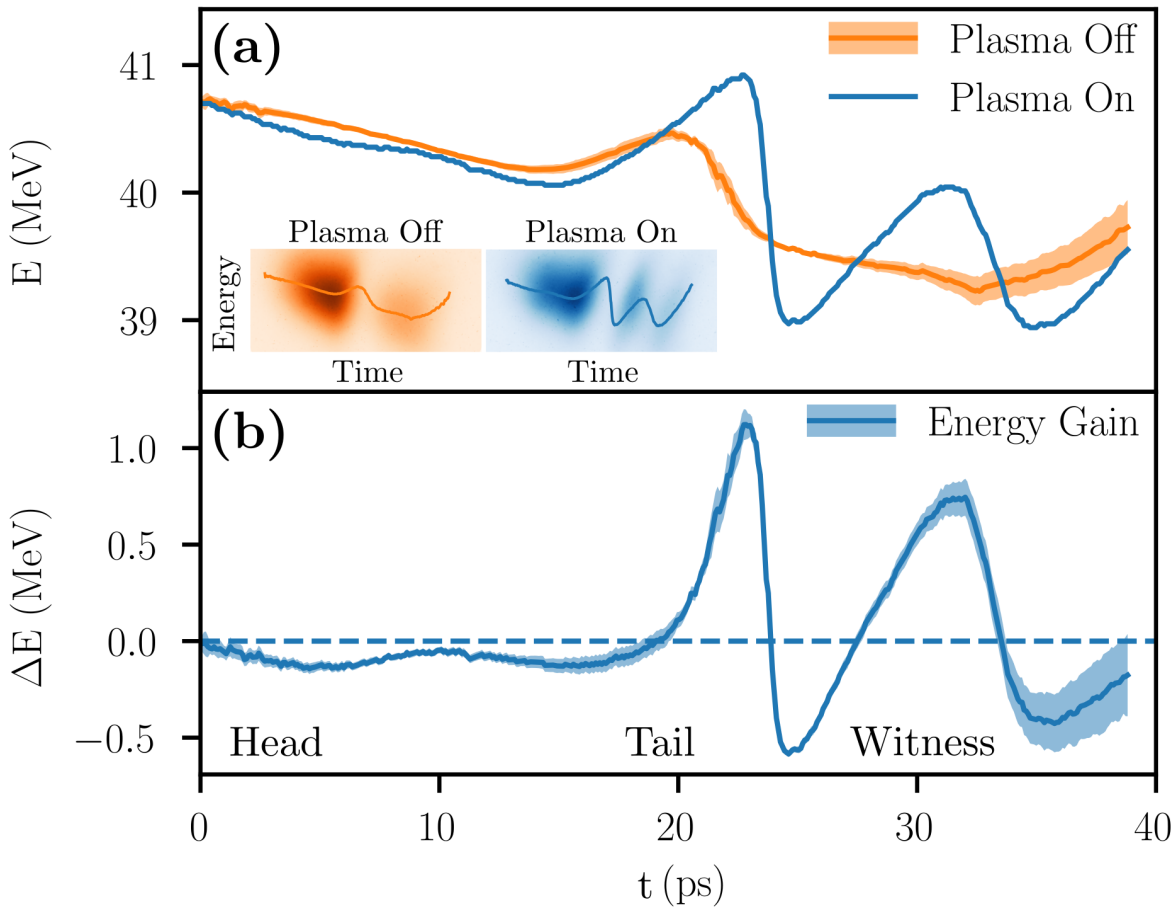

Figure 3. Example of the single shot wakefield measurement. (a) Averaged time slice energy centroid of 34 plasma off LPS measurements and a single plasma on LPS measurement. Inset: Raw YAG screen images of LPS diagnostic with individual time slice energy centroid for both plasma on and off cases. Shading denotes 1 sigma variance in the baseline slice energy centroid. (b) Calculated difference between baseline and plasma on beam slice energy. Shading denotes 1 sigma variance in $\Delta E(t)$ due to baseline measurement error.

blowout region is small compared to the plasma wavelength [22, 23]. This method is used to reconstruct the average drive current profile over the entire plasma interaction.

The measured energy gain from the drive created from the mask of Fig. 1b is shown in Fig. 4a, along with a reconstruction of the drive current profile. The reconstructed drive profile shows a nearly linear ramp over two plasma wavelengths as evidenced by the number of undulations in the decelerating wake - the separation between neighboring minima of

the wakefield in the drive is roughly equal to the plasma wavelength. In the case shown, a separation of 10 ps corresponds to a plasma wavelength of 3 mm and thus an average plasma density of 1.3 x 10^{14} cm^{-3}.

In contrast to the drive region, the observed energy modulation of the witness shows clear evidence of a nonlinear plasma wakefield response. As shown in simulation (Fig. 2) the nonlinear rarefaction and subsequent collapse of plasma electrons to the beam axis produces a characteristic sawtooth longitudinal wakefield [25]. This wakefield form is evident in the witness bunch energy gain measurement. This observation also validates theoretical predictions that the maximum accelerating potential is asymmetric with respect to the maximum decelerating potential [26]. Furthermore, we observe a transformer ratio of $\mathcal{R} = 7.8 \pm 2.3$, which is well in excess of the analytical transformer ratio expected from a similarly shaped beam in a purely single-mode wakefield [2]. This result validates theoretical predictions that a nonlinear (multi-mode) wakefield response further enhances the transformer ratio of wakefields generated via longitudinally shaped beams [27].

While linearly ramped profiles provide a way to achieve high transformer ratios, perturbations to the head of the driver may provide further benefits in wakefield excitation. For example, the ramp can be modified through the addition of a shaped head, which acts to flatten the decelerating field inside the drive beam. This is desirable, as it extends the beam-plasma interaction length by reducing drive energy spread, which, in turn, mitigates beam breakup instabilities [28] and emittance growth [29] due to betatron function mismatch. Figure 4b shows a direct observation of this effect, in a case where the head of the reconstructed drive bunch has a parabolic shape, resulting in a near uniform deceleration of electrons in the linear region of the drive. The parabolic head has a length of 6.7 ps which approaches one plasma period (8.9 ps). The plasma wavelength was calculated by measuring the time between zero crossings in the witness (n_0 = 1.6 x 10^{14} cm^{-3}) in this case, as opposed to inside the drive, due to the lack of distinct oscillations in the drive energy gain. This observation shows good agreement with analytical calculations of the wakefield [4], as uniform deceleration inside the drive occurs when the parabolic head length approaches an integer wavelength long.

In summary, we demonstrate single-shot wakefield measurements of a PWFA in the nonlinear regime, with control over drive beam shaping through use of the EEX method. The two key findings from the experiment are a recorded transformer ratio of 7.8 ± 2.3 from a

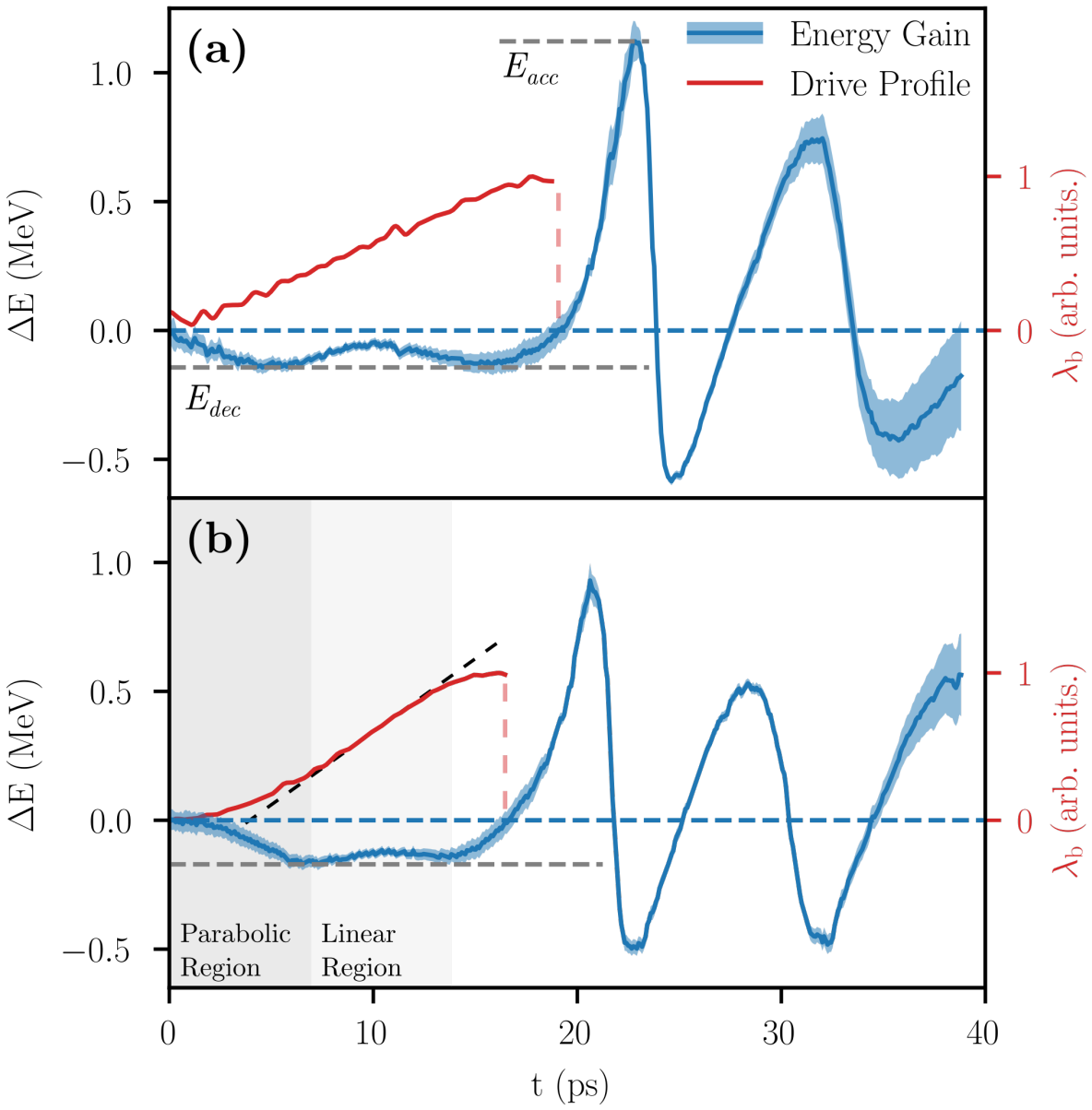

Figure 4. (Color online) (Color online) Time dependent energy gain of drive and witness beam due to plasma interaction (blue) with current profile reconstruction (red) showing (a) transformer ratio of $\mathcal{R} = 7.8 \pm 2.3$ from a near-linearly ramped drive and (b) wakefield flattening from a linear ramp (black dashed line) with a parabolic head perturbation. Shading denotes 1 sigma variance in ΔE due to baseline measurement error.

linearly ramped beam, and the observation of a near uniform decelerating field for a drive beam with a parabolic head. The former is significant because enhancing the transformer ra-

tio is a critical feature demanded in the design and deployment of next-generation wakefield accelerators [30]. The latter measurement complements and enhances this finding, because the uniform energy loss condition permits a longer sustained interaction, as one expects in an optimized transformer ratio case. These aggregate results validate the importance of experimental efforts in longitudinal beam shaping. Further, they open the door to accessing nonlinear PWFA conditions through a non-relativistic blowout, which reduces peak drive beam current requirements for ultra-short bunch wakefield excitation in high density plasmas [31]. These advantages must be weighed against possible enhancement of beam breakup effects in long beams, which is a subject of future experimental investigations.

This work is supported by the Department of Energy, Office of High Energy Physics , under contract No. DE-SC0017648.

* roussel@ucla.edu

[1] I. Blumenfeld, C. E. Clayton, F.-J. Decker, M. J. Hogan, C. Huang, R. Ischebeck, R. Iverson, C. Joshi, T. Katsouleas, N. Kirby, W. Lu, K. A. Marsh, W. B. Mori, P. Muggli, E. Oz, R. H. Siemann, D. Walz, and M. Zhou, Nature **445**, 741 (2007).

[2] K. L. F. Bane, P. Chen, and P. B. Wilson, IEEE Transactions on Nuclear Science **32**, 3524 (1985).

[3] K. L. F. Bane, P. B. Wilson, and T. Weiland, in *AIP Conference Proceedings*, Vol. 127 (AIP, 1985) pp. 875–928.

[4] F. Lemery and P. Piot, Physical Review Special Topics - Accelerators and Beams **18**, 081301 (2015).

[5] G. Andonian, S. Barber, F. H. OShea, M. Fedurin, K. Kusche, C. Swinson, and J. B. Rosenzweig, Phys. Rev. Lett. **118**, 054802 (2017).

[6] R. J. England, J. B. Rosenzweig, and G. Travish, Phys. Rev. Lett. **100**, 214802 (2008).

[7] G. Loisch, J. Good, M. Gross, H. Huck, I. Isaev, M. Krasilnikov, O. Lishilin, A. Oppelt, Y. Renier, F. Stephan, R. Brinkmann, F. Grner, and I. Will, Nuclear Instruments and Methods in Physics Research Section A: Accelerators, Spectrometers, Detectors and Associated Equipment 3rd European Advanced Accelerator Concepts workshop (EAAC2017), **909**, 107 (2018).

[8] G. Ha, M. Cho, W. Namkung, J. Power, D. Doran, E. Wisniewski, M. Conde, W. Gai, W. Liu, C. Whiteford, Q. Gao, K.-J. Kim, A. Zholents, Y.-E. Sun, C. Jing, and P. Piot, Phys. Rev. Lett. **118**, 104801 (2017).

[9] P. Piot, Y.-E. Sun, J. G. Power, and M. Rihaoui, Phys. Rev. ST Accel. Beams **14**, 022801 (2011).

[10] Q. Gao, J. Shi, H. Chen, G. Ha, J. G. Power, M. Conde, and W. Gai, Phys. Rev. Accel. Beams **21**, 062801 (2018).

[11] Q. Gao, G. Ha, C. Jing, S. Antipov, J. Power, M. Conde, W. Gai, H. Chen, J. Shi, E. Wisniewski, D. Doran, W. Liu, C. Whiteford, A. Zholents, P. Piot, and S. Baturin, Phys. Rev. Lett. **120**, 114801 (2018).

[12] G. Loisch, G. Asova, P. Boonpornprasert, R. Brinkmann, Y. Chen, J. Engel, J. Good, M. Gross, F. Grner, H. Huck, D. Kalantaryan, M. Krasilnikov, O. Lishilin, A. M. de la Ossa, T. J. Mehrling, D. Melkumyan, A. Oppelt, J. Osterhoff, H. Qian, Y. Renier, F. Stephan, C. Tenholt, V. Wohlfarth, and Q. Zhao, Phys. Rev. Lett. **121**, 064801 (2018).

[13] A. Halavanau, G. Qiang, G. Ha, E. Wisniewski, P. Piot, J. Power, and W. Gai, Phys. Rev. Accel. Beams **20**, 103404 (2017).

[14] G. Ha, M. Cho, W. Gai, K.-J. Kim, W. Namkung, and J. Power, Phys. Rev. Accel. Beams **19**, 121301 (2016).

[15] R. Roussel, G. Andonian, M. Conde, D. Doran, G. Ha, W. Lynn, J. Power, J. Rosenzweig, J. Seok, C. Whiteford, and E. Wisniewski (JACOW Publishing, Geneva, Switzerland, 2019) pp. 3778–3781.

[16] R. Roussel, G. Andonian, C. Hansel, G. Lawler, W. Lynn, N. Majernik, R. Robles, K. Sanwalka, E. Wisniewski, and J. Rosenzweig, Instruments **3**, 48 (2019).

[17] S. Chen and T. Sekiguchi, Journal of Applied Physics **36**, 2363 (1965).

[18] G. R. Lynch and O. I. Dahl, Nuclear Instruments and Methods in Physics Research Section B: Beam Interactions with Materials and Atoms **58**, 6 (1991).

[19] D. P. Grote, A. Friedman, J. Vay, and I. Haber, AIP Conference Proceedings **749**, 55 (2005).

[20] L. Wartski, S. Roland, J. Lasalle, M. Bolore, and G. Filippi, Journal of Applied Physics **46**, 3644 (1975).

[21] N. Barov and J. B. Rosenzweig, Phys. Rev. E **49**, 4407 (1994).

[22] W. Lu, C. Huang, M. Zhou, W. B. Mori, and T. Katsouleas, Phys. Rev. Lett. **96**, 165002

(2006).

[23] W. Lu, C. Huang, M. M. Zhou, W. B. Mori, and T. Katsouleas, Physics of Plasmas **12**, 063101 (2005).

[24] R. Roussel, G. Andonian, M. Conde, D. Doran, G. Ha, W. Lynn, J. Power, J. Rosenzweig, J. Seok, C. Whiteford, and E. Wisniewski, .

[25] J. B. Rosenzweig, B. Breizman, T. Katsouleas, and J. J. Su, Physical Review A **44**, R6189 (1991).

[26] J. B. Rosenzweig, Phys. Rev. A **38**, 3634 (1988).

[27] J. Rosenzweig, IEEE Transactions on Plasma Science **15**, 186 (1987).

[28] A. Mosnier, *Instabilities in linacs* (CERN, 1995).

[29] T. Mehrling, J. Grebenyuk, F. S. Tsung, K. Floettmann, and J. Osterhoff, Phys. Rev. ST Accel. Beams **15**, 111303 (2012).

[30] *Advanced Accelerator Development Strategy Report: DOE Advanced Accelerator Concepts Research Roadmap Workshop*, Tech. Rep. (USDOE Office of Science, Washington, DC (United States), 2016).

[31] M. J. Hogan, T. O. Raubenheimer, A. Seryi, P. Muggli, T. Katsouleas, C. Huang, W. Lu, W. An, K. A. Marsh, W. B. Mori, C. E. Clayton, and C. Joshi, New J. Phys. **12**, 055030 (2010).